Applied Magnetic Resonance
https://doi.org/10.1007/s00723-020-01281-3

Applied
Magnetic Resonance

ORIGINAL PAPER

NMR Study of Spin Dynamics in V_7Zn and V_7Ni Molecular Rings

F. Adelnia[1] · P. Arosio[1] · M. Mariani[2] · F. Orsini[1] · A. Radaelli[3] · C. Sangregorio[4] · F. Borsa[2] · J. P. S. Walsh[5] · R. Winpenny[6] · G. Timco[4] · A. Lascialfari[1,2,7]

Received: 1 July 2020 / Revised: 25 September 2020 / Accepted: 30 September 2020

Abstract

We present a ^{1}H NMR investigation of spin dynamics in two finite integer spin molecular nanomagnetic rings, namely V_7Zn and V_7Ni. This study could be put in correlation with the problem of Haldane gap in infinite integer spin chains. While V_7Zn is an approximation of a homometallic broken chain due to the presence of $s=0$ Zn^{2+} ion uncoupled from nearest neighbor V^{2+} $s=1$ ions, the V_7Ni compound constitutes an example of a closed periodical $s=1$ heterometallic chain. From preliminary susceptibility measurements on single crystals and data analysis, the exchange coupling constant J/k_B results in the order of few kelvin. At room temperature, the frequency behavior of the ^{1}H NMR spin–lattice relaxation rate $1/T_1$ allowed to conclude that the spin–spin correlation function is similar to the one observed in semi-integer spin molecules, but with a smaller cutoff frequency. Thus, the high-T data can be interpreted in terms of, e.g., a Heisenberg model including spin diffusion. On the other hand, the behavior of $1/T_1$ vs temperature at different constant fields reveals a clear peak at temperature of the order of J/k_B, qualitatively in agreement with the well-known Bloembergen–Purcell–Pound model and with previous results on semi-integer molecular spin systems. Consequently, one can suggest that for a small number N of interacting $s=1$ ions ($N=8$), the Haldane conjecture does not play a key role on spin dynamics, and the investigated rings still keep the quantum nature imposed mainly by the low number of magnetic centers, with no clear topological effect due to integer spins.

1 Introduction

The ground state of an infinite antiferromagnetic (AFM) spin 1D chain is gapless for the case of semi-integer spins [1]. On the other hand for integer spins, the AFM ground state of an infinite chain is separated by a finite gap from the first excited

✉ M. Mariani
manuel.mariani@unipv.it

Extended author information available on the last page of the article

Published online: 17 October 2020

state (Haldane prediction) [2]. This is an important result both for the general standpoint of topological effects in statistical mechanics and for the specific applications to magnetism. On the other hand, in the last decades, chemists and physicists have developed the field of single molecule magnets (SMM) [1] that represent ideal models to study magnetism on a limited and controlled finite number of spins, mainly in zero and one dimension. Their investigation has led to the discovery of new fundamental physics phenomena, at the border between quantum and classical framework, e.g., quantum tunneling [1, 3–7] and coherence, quantized transport and quantum information processing (QIP), but also possible applications in the fields of data storage and quantum computation [1] (for quantum computation/information, see e.g., Refs. [8, 9]); for data storage see, e.g., Refs. [10, 11]).

A particular class of molecular nanomagnets (MNMs) is represented by magnetic molecular rings composed of magnetic ions coupled by strong antiferromagnetic (super-) exchange interactions and placed on an almost coplanar circular arrangement. For the semi-integer spin "ring" systems (that can be thought as a closed periodic chain), the low temperature energy levels' scheme is approximately described by the Landè formula $E(S) = (P/2)S(S+1)$, where $P = 4\ J/N$. The presence of a finite number of spins implies a discrete energy levels' structure that follows such formula, and thus a gap between the ground state and the first excited state, leading to a gapless ground state in the limit of N going to infinite. In the case of an integer spin ring, i.e., a system formed by a finite number of integer spins, there is again a discrete levels' structure and a gap between the ground state and the first excited state. However, in this case by increasing the number of spins, one should find a significant deviation from Lande's rule signaling the approach to the infinite spin chain, where the Haldane gap is present. It seems thus of interest to initiate a systematic investigation of integer spin rings to find out if one can see a possible different behavior in the magnetic properties and the spin dynamics between the integer spin and the semi-integer spin systems, even in the case of a finite number of magnetic ions in the ring (or chain). It should be further noted that future investigations could regard systems, other than those studied here, where the ring (or finite size chain) length, number of ions and parity (odd or even), topology (open or closed) and kind of ions (heterometallic or homometallic compounds) are changed.

Recently, two different integer-spin AFM rings with general formula $[\{(CH_3)_2NH_2\}V_7MF_8(O_2C^tBu)_{16}]\cdot 2C_7H_8$, M = Ni and Zn have been synthesized. In Ref. [12] the synthesis and structural characterization of the two compounds are reported. It is worth noting that, unfortunately, it was not possible to have a stable V_8 ring due to undesired oxidation, and thus a direct comparison of homometallic semi-integer and integer spin systems is not currently possible. V_7Ni is characterized by a total spin $S_T = 0$ in the ground state, resulting from nearest-neighbor AFM interactions between V^{2+} ($s = 1$) ions and the substituting ion Ni^{2+} ($s = 1$). In the case of V_7Zn, as the substituting ion is Zn^{2+} ($s = 0$), no magnetic interaction occurs between V^{2+} and Zn^{2+}, resulting in an uncompensated total $S = 1$ ground state. Consequently, V_7Ni is a heterometallic "closed" ring and V_7Zn can be considered a "broken" ring which mimics a short segment of seven integer spins. Both rings appear suitable to investigate the spin dynamics in integer spin rings, to be compared to the one in semi-integer spins.

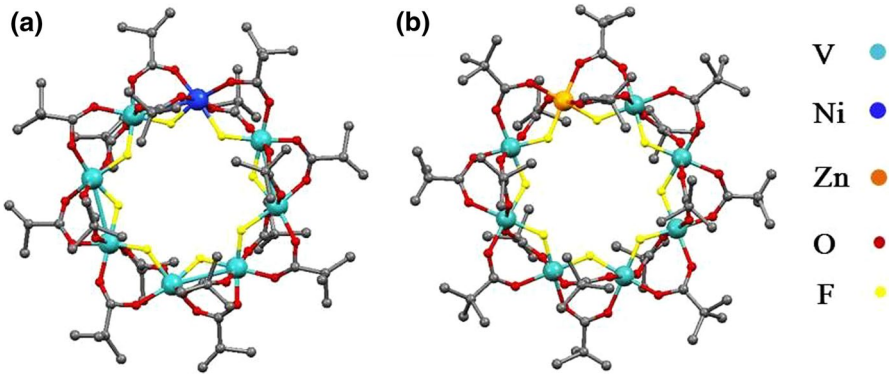

Fig. 1 **a** V_7Ni and **b** V_7Zn molecular rings. Hydrogen atoms, dimethyl ammonium cation, and solvent toluene molecules are omitted for clarity

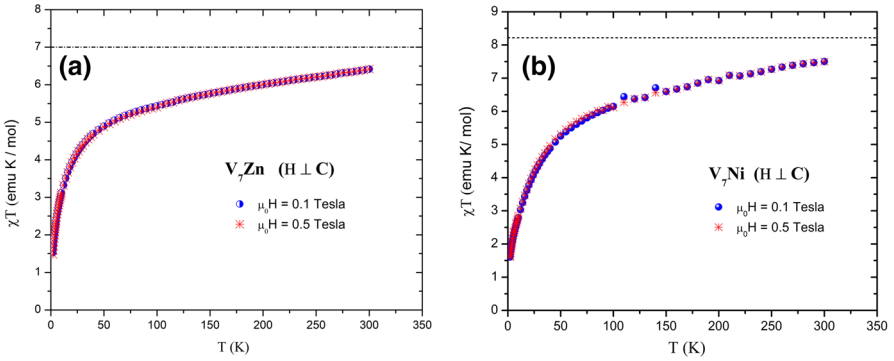

Fig. 2 χT as a function of temperature for external magnetic field $H \perp c$ (with c the axis perpendicular to the plane of the ring), at field values $\mu_0 H = 0.1$, and 0.5 T, for **a** V_7Zn and **b** V_7Ni single crystals. The dashed lines correspond to the high-temperature effective Curie constant limit

A sketch of the V_7Zn and V_7Ni ring structure is shown in Fig. 1.

In Fig. 2, we report the experimental molar magnetic susceptibility χ multiplied by temperature as a function of temperature, measured at two different magnetic fields $\mu_0 H = 0.1$ and 0.5 T, applied perpendicularly to the c molecular axis which lies normal to the plane of the rings. The χT product in both rings approaches at high temperature the value expected for a simple paramagnet composed of independent moments pertaining to the single V^{2+} magnetic ions. At low temperature, the drop of the effective Curie constant χT corresponds to the gradual depopulation of the excited states toward the ground state energy level. A complete presentation of the magnetic properties and the fits of the magnetization curves will be published separately (F. Adelnia et al., unpubl.).

In this paper, we present and discuss only the results of ^1H nuclear magnetic resonance and relaxation in the V_7Ni and V_7Zn rings. A large body of literature describing the spin dynamics obtained by NMR in magnetic molecules [13, 14] and

in particular in the semi-integer spin ring systems exists [15–20]. In contrast, the importance of spin dynamics in integer spin ring systems has not been well recognized by the NMR community, and no paper, to our knowledge, has been published. Here, we report the first ^{1}H NMR investigation of integer spin Vanadium-based rings, and use the results of semi-integer spin systems as a point of comparison. We present the proton NMR results, separating the presentation of the room temperature results (Sect. 3) from the results at low temperature (Sect. 4). Section 2 contains a brief discussion of the experimental setup and Sect. 5 the summary and conclusions. It will be shown that the nuclear spin–lattice relaxation rate $1/T_1$ displays a room temperature behavior vs. frequency (i.e., field) well interpretable in terms of a Heisenberg model of spin diffusion and/or a finite size model of periodical spin chains (rings). The same quantity studied as a function of temperature at fixed magnetic field is characterized by a peak occurring at temperatures of the order of the exchange coupling constant J/k_B. Thus, the slowing down of the relaxation dynamics results similar to system rings constituted of semi-integer spins.

2 Experimental Details

^{1}H NMR measurements were performed on single crystals as a function of temperature ($1.6 \leq T \leq 300$ K) at different magnetic fields $\mu_0 H = 0.5$, 1.5, ~3 and ~6 T, and as a function of magnetic field ($0.3 < \mu_0 H < 9$ T) at room temperature, for $H \perp c$. To control the temperature, we used two different cryostats: a dynamic/static continuous flow cryostat for the temperature range from room temperature down to 4.2 K, and a bath cryostat from 4.2 to 1.6 K. To set the value of magnetic field that was needed in NMR measurements, two different setups were used: an electromagnet for the lower magnetic field range ($0.3 < \mu_0 H < 1.7$ T), and a superconducting-magnet for the higher range ($2 < \mu_0 H < 9$ T). ^{1}H NMR measurements, including $1/T_1$, $1/T_2$ and NMR spectra, were obtained by using a standard TecMag Fourier transform pulse NMR spectrometer.

The value of the nuclear spin–lattice relaxation rate (NSLR), $1/T_1$, was determined by monitoring the recovery of the longitudinal nuclear magnetization measured by means of a reading $[\pi/2]_x - \Delta - [\pi/2]_y$ pulse sequence that follows a saturation comb of $[\pi/2]$ radiofrequency (*rf*) pulses, Δ being a very short separation time interval. The length of the *rf* comb was adjusted to ensure the best initial saturation condition at the different temperatures and resonance frequencies. Every recovery curve was then obtained by measuring the spin echoes at progressively longer delay times between the comb and the $[\pi/2]_x - [\pi/2]_y$ reading sequence. It is worth noting that the spin echo signal is the response of the whole set of protons of the irradiated line after a certain delay time and each $1/T_1$ data point at fixed temperature/field is extracted from one recovery curve.

Transverse relaxation measurements, $1/T_2$, were performed mainly by using a $[\pi/2]_x - \tau - [\pi/2]_y$ solid-spin-echo pulse sequence. The decay curves were acquired by measuring the echo signal at progressively longer τ delay time. In essence, a

curve of $M_{xy}(t)$ gives the irreversible decay of the transverse nuclear magnetization in the x–y plane.

In the case of ^1H NMR spectra, different strategies were employed. For the high and intermediate temperature regions where the whole NMR line could be excited by a single *rf* pulse, the proton NMR spectra were simply obtained from the Fourier transform of half of the echo signal. On the other hand, in the low temperature region, the whole NMR line could not be irradiated by means of only a single *rf* pulse and thus a field-sweep method was adopted to collect the whole spectra. In this latter technique, the radio frequency is kept fixed, while the applied magnetic field is swept over a selected range around the resonance Larmor field of the bare nucleus. The experimental point of the spectrum is given, at any field value, by the integral of the acquired spin–echo signal. Still at low termperature, in some cases we employed the frequency-sweep technique alternative to the magnetic field sweep. In this method, the magnetic field is kept fixed while the frequency is manually swept over a selected range around the Larmor frequency. The echo signal is then acquired after tuning and matching at the desired frequency. Finally, by plotting all the NMR data points obtained from the Fourier transform of each echo signal (corresponding to different frequencies), one can obtain the complete spectrum.

One should take into account that the experimental results are undoubtedly affected by several different errors mainly due to electronic noise, signal integration, and the evaluation of the signal intensity at infinite delay time in T_1 measurements (i.e., the measure of the equilibrium nuclear magnetization). Since the statistical study of the experimental error is unfeasible, we have used an average estimated experimental uncertainty for all data points of $\pm 5\%$.

3 Room Temperature NMR Results and Discussion

The aim of the present high-temperature ($T \sim 300$ K) work is to study the spin dynamics of the AFM rings V_7Ni and V_7Zn, by determining the behavior of the spectral density $S(\omega)$ of the electronic spin fluctuations, to see if there is a detectable difference in the behavior of the "quantum" integer spin ring with respect to the ($s \geq 3/2$) semi-integer spin rings. The quantity $S(\omega)$ is the Fourier transform of the electronic spin–spin correlation function and its curve vs frequency ω represents the "renormalized" number of electronic spins fluctuating at different frequencies, and thus the so-called spin dynamics. One of the most direct experimental measurements of $S(\omega)$ comes from the NSLR data. In fact, the nuclei couple to the magnetic electrons by means of the hyperfine interaction and are thus sensitive to the fluctuations of the electron spins. Since in the weak collision approach the NSLR is proportional to the spectral density at the Larmor frequency $S(\omega_L)$ [21, 22], one can probe directly the low-frequency behavior of the spectral density by performing NSLR measurements as a function of applied magnetic field (i.e., resonance frequency ω_L).

As said above, the NSLR was measured as a function of magnetic field at room temperature on a single crystal, for $H \perp c$. At this temperature, the nuclear magnetization recovery curves showed a single exponential behavior and therefore T_1 values were simply extracted by fitting the recovery with a single exponential

function. The experimental results are shown in Fig. 3. Data were analyzed on the basis of two spin dynamics models mentioned later on.

Both models start from a classical approximation. In fact, since $T = 300$ K is much larger than the AFM exchange interaction of the spins in the rings, one can use a classical approximation to calculate the spin dynamics. For an infinite AFM isotropic Heisenberg chain, several theoretical and numerical calculations have demonstrated that at long times there is a persistence of the spin–spin correlation function (CF) due to the conservation of the total spin value, whereby the slow decay of the CF in 1D can be described by a spin diffusion process [23–26]. As a consequence, the Fourier transform (FT) of the CF (i.e., the spectral density $S(\omega)$ of the electronic spin fluctuations) displays an enhancement at low frequency (long times). The first experimental confirmation of spin diffusion was done in a Heisemberg AFM spin chain containing Mn ions [27, 28]. It should be further noted that in a spin ring or a short spin segment the CF, after an initial fast decay due to the AFM exchange interaction, reaches a constant value inversely proportional to the number N of spins, as long as the total spin value is conserved [29, 30]. In both the infinite and in the finite chain or ring the CF eventually goes to zero due to anisotropic terms in the spin–spin interaction which do not conserve the total spin. The time at which the CF decays to zero is called cutoff time. If we refer to the spectral density (i.e., the Fourier transform of the CF), the cutoff frequency is the frequency at which the low-frequency enhancement of $S(\omega)$ levels off [27–30].

The first spin dynamics model is the one describing the CF of the vanadium spins with an initial fast decaying component determined by the strong exchange interaction J, followed by a plateau in the CF and a cutoff function whose FT in the frequency domain, $S(\omega)$, is approximated by a Lorentzian function of width ω_{cutoff}. The NSLR, which is proportional to the FT $S(\omega_L)$ of the CF, can then be expressed as [13, 14]:

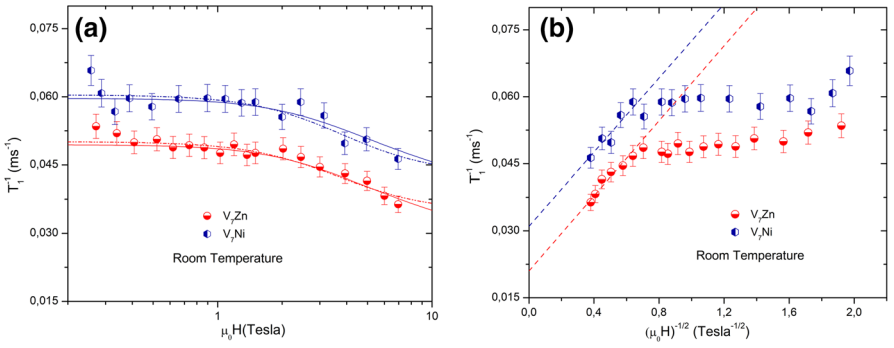

Fig. 3 Proton NSLR, $1/T_1$, at room temperature for V_7Zn and V_7Ni. **a** The data are plotted as a function of the external magnetic field. The dashed lines are the best fits according to Eq. 1 with the set of parameters listed in Table 1. The solid lines are the best fits according to the 1D spin diffusion model, i.e., Equation 2, with the set of fitting parameters listed in Table 2; **b** the data are plotted as a function of the inverse square root of the applied magnetic field. The dashed straight lines are the limiting behavior of Eq. 2 for $H_c = 0$, i.e., Equation 3

Table 1 The fitting parameters of Eq. 2 for different integer spin systems, see Fig. 3a

AFM ring	Type/ground state	A (m s^{-1})	H_c (T)	C (m s^{-1})
V_7Zn	Open/$S_T=1$	0.015 (0.005)	3.65 (0.4)	0.35 (0.01)
V_7Ni	Closed heterom./$S_T=0$	0.017 (0.005)	3.8 (0.4)	0.043 (0.01)

Table 2 The fitting parameters of Eq. 3 for different integer spin systems, see Fig. 3b

AFM ring	Type/ground state	P ($T^{1/2}$ m s^{-1})	H_c (T)	Q (m s^{-1})
V_7Zn	Open/$S_T=1$	0.032 (0.005)	3.2 (0.4)	0.024 (0.01)
V_7Ni	Closed heterom./$S_T=0$	0.032 (0.005)	3.3 (0.4)	0.034 (0.01)

$$\frac{1}{T_1} = \frac{A}{1+\left(H/H_c\right)^2} + C(\mathrm{ms})^{-1}, \tag{1}$$

where $H_c = \omega_{\mathrm{cutoff}}/\gamma_N$ is the cutoff field (γ_N = nuclear gyromagnetic ratio), ω_{cutoff} is the cutoff frequency and C comes from the contribution of the first fast decay of the CF, and ω_{cutoff} is the cutoff frequency. As seen in Fig. 3a dashed lines, the model fits well the data with the parameters shown in Table 1.

The second model is the one described by a CF which after an initial fast decay has a slow decaying part at long times due to the spin diffusion, with a cutoff time due to terms in the Hamiltonian which do not conserve the total spin value. The model has been applied successfully to infinite AFM isotropic Heisenberg chains [27, 28]. The NSLR is expressed by:

$$\frac{1}{T_1} = P\left\{\frac{\left(H_c^2+H^2\right)^{1/2}+H_c}{\left[H_c^2+H^2\right]}\right\}^{1/2} + Q, \tag{2}$$

where H_c is the cutoff field as in Eq. 1, Q is the contribution of the fast initial decay of the CF (same as C in Eq. 1) and $P = B/2\pi(2D\gamma_e)^{1/2}$, where D is the spin diffusion constant in rad Hz and B is the average square of the hyperfine interactions between nuclei and electrons in units of (rad Hz)^2. Equation 2 also fits well the data in Fig. 3a, solid lines, with the parameters in Table 2.

To see if there is a limited field range in which the NSLR is due to spin diffusion in the ring, one can plot the data as a function of$H^{-1/2}$, as depicted in Fig. 3b. A straight line in such a plot corresponds to the spin diffusion range as given by Eq. 2 in the limit of $H_c = 0$:

$$\frac{1}{T_1} = \mathrm{PH}^{-1/2} + Q. \tag{3}$$

As one can see from the inspection of the fitting parameters and the experimental data, the results are similar in the two systems, with a small difference

in the C and Q values. The main result is that the cutoff field is "low" and this allows to observe that spin diffusion occurs in a small field range, as shown by the straight line fitting high fields data in Fig. 3b. When one compares the results for the two integer vanadium rings with the results in rings of semi-integer spins [13, 14], e.g., Cr8, Fe6, Fe10, Cr7Cd and Cr8Zn, one finds that the results are similar except for the lower cutoff field observed in the vanadium rings. The lower cutoff field in V rings could be due to the different local anisotropy of V^{2+} ions with respect to, e.g., Cr^{2+} ions, and/or the difference between the spin values, i.e., $s = 1$ for V^{2+} ions and $s = 3/2$ for Cr^{2+} ions, and/or a different intermolecular interaction. It is important to remark that the spin diffusion seems to be present both in closed and open heterometallic rings.

A general conclusion of the NMR room temperature study of the integer spin rings is that no detectable difference can be observed in the spin dynamics with respect to the semi-integer spin rings. Moreover, the two proposed models that describe the spin dynamics work both correctly. Future theoretical work should help to distinguish the most appropriate one.

4 Low Temperature NMR Results and Discussion

As the temperature is lowered and becomes comparable to the magnetic exchange interaction J ($k_B T \approx J$), strong correlations among the magnetic moments start building up. Thus at low temperature, the spin dynamics is dominated by the enhancement and slowing down of collective fluctuations in a way similar to what happens in a magnetic system as one approaches a magnetic phase transition [31]. Even if no phase transition takes place in our finite size magnetic rings, the slowing down of the fluctuations, occurring when the temperature decreases, generates an enhancement in the NSLR. Moreover, when by diminishing T the characteristic frequency of the magnetization fluctuations reaches a value of the order of the nuclear Larmor frequency ω_L, the NSLR diplays a maximum followed by a subsequent decrease when the temperature is further lowered. This behavior, including a peak in NSLR, has been observed in all the MNMs and magnetic rings investigated so far [13, 14]. However, the magnetic rings investigated are all made up of semi-integer spins and thus it seems of interest to investigate integer spin rings like V_7Zn and V_7Ni to see if any difference in the spin dynamics can be detected.

Before presenting and discussing the results of proton NSLR, it is important to show the effects generated, on lowering temperature, on other proton NMR parameters, namely the ^1H NMR line width, the transverse nuclear relaxation rate $1/T_2$ and the signal intensity. These effects will have to be taken into consideration in the analysis of the NSLR, which is the relevant parameter conveying information of the spin dynamics. (In the present report we summarize the results on the NMR parameters. For a complete analysis and discussion of the same, see Ref. [32].) The data were collected on a single crystal with H parallel to the molecular rings' plane at different applied magnetic fields (i.e., $H \perp c$).

4.1 *^1H NMR Line Width*

The results for the proton line width measured as the full width at half maximum (FWHM) are shown in Fig. 4 as a function of temperature for different applied magnetic fields. Note that due to the large FWHM observed in V_7Zn at 3 and 6 T, at very low temperature the frequency-sweep technique is used to measure correctly the broadening of the absorption spectrum.

As shown in Fig. 4, the NMR line width increases as the temperature is lowered down to about 20 K, and in this temperature range it is proportional to the paramagnetic susceptibility since the line is inhomogeneously braodened by the distribution of local fields at the proton nuclei sites due to the hyperfine interaction of the proton with the vanadium spins. At lower temperatures, the system is no longer a simple paramagnet because of the strong AFM exchange interaction (see Fig. 2) that increases progressively the spin–spin correlation. In fact at low temperature, the magnetization of the rings is due to the molecular population of the low-lying discrete magnetic energy states governed by the Boltzmann law, and the NMR line width is no longer proportional to the magnetic susceptibility [32]. It is noted that the rigid lattice line width due to the nuclear dipolar interaction is only about 20 kHz and is thus negligible compared to the inhomogeneous broadening due to the paramagnetism of the system.

4.2 *Transverse Relaxation Rate $1/T_2$*

The temperature dependence of the transverse relaxation rate in V_7Zn and V_7Ni is shown in Fig. 5 for different applied magnetic fields.

In a diamagnetic solid or a paramagnetic solid made of independent spins, the spin–spin relaxation rate $1/T_2$ is due to the nuclear dipolar interaction and is of the order of the rigid lattice line width. As in our case, the nuclear dipolar interaction yields a line width of the order of 20 kHz (see FWHM data for $T > 100$–150 K, Fig. 4); this corresponds to a transverse relaxation rate of about 50 μs, which is indeed the value observed in Fig. 5 at $T > 100$–150 K. As the temperature is lowered

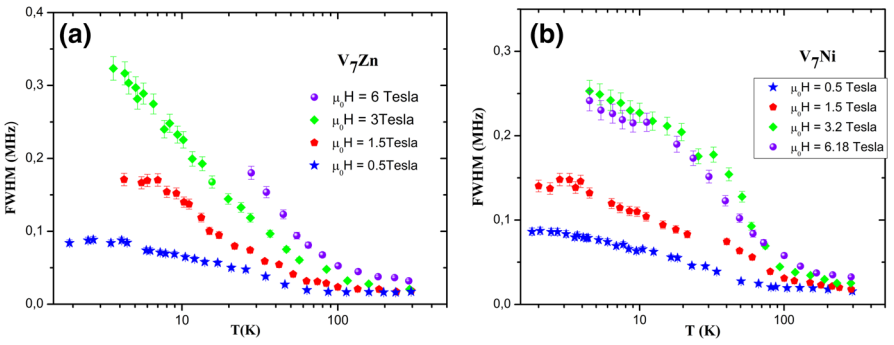

Fig. 4 Proton line width vs. temperature at different applied magnetic fields in **a** V_7Zn and **b** V_7Ni

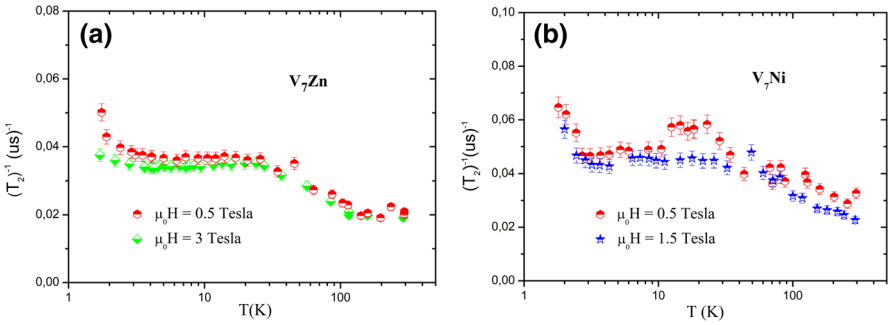

Fig. 5 Temperature dependence of spin–spin relaxation rate, $1/T_2$, for **a** V_7Zn at $\mu_0 H = 0.5$ and 3 T **b** V_7Ni at $\mu_0 H = 0.5$ and 1.5 T

below 100–150 K, the slowing down of the magnetization fluctuations introduces a further term in the spin–spin relaxation rate of dynamic nature due to the interaction of the proton nuclei with the vanadium spins. In the weak collision limit, within the fast motion approximation, where the transverse relaxation rate can be expressed in terms of the spectral density of the fluctuating hyperfine fields at zero frequency, the dynamic contribution to the transverse relaxation rate can be expressed as [26]:

$$\frac{1}{T_2} = \gamma_N^2 \left\langle \delta H_z^2 \right\rangle \tau(T) = \gamma_N^2 \frac{\left\langle \delta \mu_e^2 \right\rangle}{r^6} \tau(T), \tag{4}$$

where δH_z represents the local longitudinal field fluctuations originating from a magnetic moment μ_e at a distance r from the proton spin, and τ is the correlation time (i.e., the inverse of the correlation frequency ω_c) which is determined by the dynamics of the exchange coupled magnetic ions. When the correlation time in Eq. 4 becomes gradually longer with decreasing temperature, then the relaxation rate $1/T_2$ becomes larger as can be seen in Fig. 5. This enhancement of $1/T_2$ at low temperature has important consequences on the detection of the NMR signal as discussed in the following subsection.

4.3 NMR Signal Intensity

In most of MNMs and magnetic rings it has been observed that the proton NMR signal loses intensity on lowering the temperature [13, 14]. This phenomenon, which has been observed also in other solids, is called "wipe-out" effect and is attributed to the combination of a strong hyperfine coupling of nuclei to the electronic spin and a slowing down of the fluctuations of the magnetic moment of the ions. In fact, the slowing down of the fluctuations of the magnetization of the molecule produces a T_2 shortening (and a corresponding shortening of T_1). When T_2 becomes very short, the decay of the transverse nuclear magnetization occurs in a time shorter than the detection time, τ_d, of the spectrometer. The minimum value for τ_d (i.e., the dead time of the instrument) is about 10 μs, below which the true observation of the NMR

echo signal is not possible due to the instrumental limits and the signal is wiped out. The "wipe-out" effect is observed also in the vanadium rings as shown in Fig. 6.

To explain quantitatively the "wipe-out" effect in magnetic molecules and rings, an approximate simple model has been proposed [33]. In short, this model is based on an assumption about the temperature dependence of T_2 whereby, when T_2 crosses the limiting value of τ_d, the NMR signal is no longer measurable. Because the protons are distributed at different distances from the magnetic ion, the critical value τ_d is reached by all proton sites, with the ones closer to magnetic ions being wiped out first, generating a gradual loss of the NMR signal intensity. It can be used to fit the data in the vanadium rings, but we will not report the details of the analysis as they are not essential for the purpose of the present investigation [32].

4.4 *Longitudinal Relaxation Rate $1/T_1$*

We turn now to the results of NSLR $1/T_1$ versus temperature. The longitudinal magnetization recovery curves in both V_7Ni and V_7Zn showed a single exponential behavior from high temperature down to 50 K for all magnetic fields. For lower temperatures, the recovery curves revealed a bi-exponential behavior composed of a fast and a slow relaxation component, due to the presence of nonequivalent groups of ^1H nuclei. This behavior is due to the different hyperfine field experienced by ^1H nuclei in nonequivalent crystallographic sites that give rise to different "average" values of the relaxation rates. However, it is worth noticing that the first exponential component of the nuclear magnetization longitudinal recovery curves, the so-called fast component, has a higher weight from more than 95% at room temperature to about 60% at the lowest temperature $T \sim 1.6$ K for all applied fields. This is an important remark, since it means that the T_1 values extracted from the fast component represent an average of the relaxation times of the majority of protons. It has to be remarked that the variation of the percent weight of the different relaxation components is related to the "wipe-out" effect.

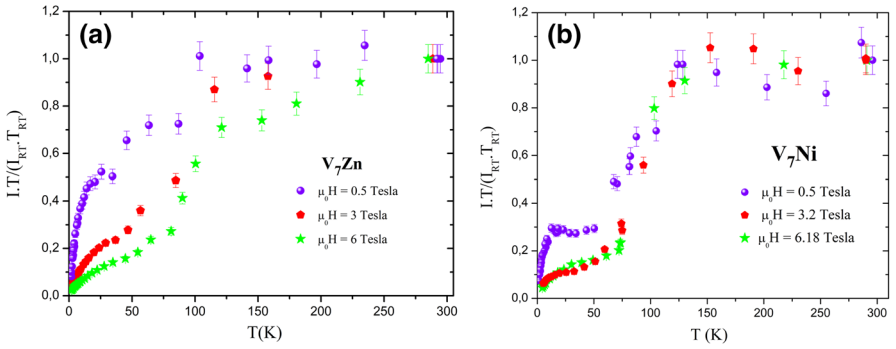

Fig. 6 ^1H NMR signal intensity times the temperature, normalized to the room temperature value, as a function of temperature for **a** V_7Zn at $\mu_0 H = 0.5$, 3, and 6 T **b** V_7Ni at $\mu_0 H = 0.5$, 3.2, and 6.18 T

Before proceeding with experimental data analysis, it should be reminded that in the weak collision approach, where the hyperfine interaction is treated as a perturbation, the NSLR can be written as [16–18, 34, 35]:

$$\frac{1}{T_1} = A\chi T \frac{\omega_c(T)}{\omega_c^2(T) + \omega_L^2}, \tag{5}$$

where A is the geometric part of the squared hyperfine interaction, χT represents the average of the effective squared electronic magnetic moment, ω_L is the nuclear Larmor frequency and $\omega_c(T)$ represents the correlation frequency. Equation 5 is called BPP-like equation because it is similar to the well-known Bloembergen–Purcell–Pound [36] formula used to fit the relaxation data in liquids. Under some simplifying assumption, in the framewrok of the quantum perturbation theory it can be derived to describe the NSLR of a magnetic system having a magnetic susceptibility χ [34, 35]. The key assumption is that the correlation function (CF) of the electronic magnetization can be described by a simple exponential function dominated by a single correlation time $\tau(T) = 1/\omega_c(T)$. Thus, as derived from the perturbation theory and presented in Eq. 5 [21, 22], while the $A\chi T$ term represents the average of the squared hyperfine field (determined by the system geometry and the effective squared electronic moment), the term including $\omega_c(T)$ is the FT of the CF, i.e., the spectral density of the electronic spin fluctuations (the spin dynamical part of $1/T_1$). Equation 5 has been used successfully to fit the NSLR in MNMs and rings [13, 14].

The experimental temperature dependence of the fast component of the longitudinal relaxation rate divided by χT is shown in Fig. 7 for the two vanadium rings (symbols). As one can see, the temperature dependence of the $1/(T_1\chi T)$ data for both rings is characterized by a peak centered at around $3 \div 6$ K. The position and height of the peaks are reported in Table 3(a) and (b) for V_7Zn and V_7Ni, respectively. The peak in $1/(T_1\chi T)$ decreases in height and shifts toward higher temperatures as the magnetic field is increased. It can be noticed that the peak appears at temperatures of the order of $T \sim J/k_B$. Since in the case of antiferromagnetic (AFM) rings there is only a finite number of magnetic ions, the nearest-neighbor exchange constant J can be obtained from the fit of the magnetization measurements by using the PHI

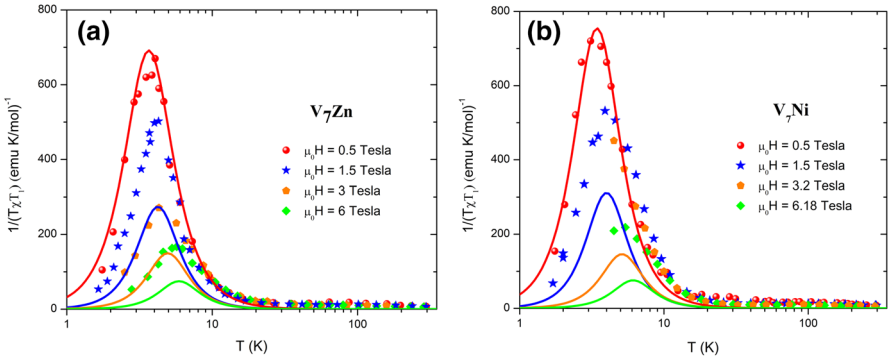

Fig. 7 Temperature dependence of the proton NSLR divided by χT, for different applied magnetic fields for **a** V_7Zn and **b** V_7Ni. The lines are the best fit curves according to Eq. 5 as explained in the text

Table 3 Position and height of the NSLR rate divided by χT for (a) V_7Zn and (b) V_7Ni spin-1 AFM rings

(a) V_7Zn		
Field (T)	T_{peak} (K)	Height (emu S K $mol^{-1})^{-1}$
$\mu_0H=0.5$	3.7 (0.4)	663 (10)
$\mu_0H=1.5$	4.2 (0.4)	500 (10)
$\mu_0H=3$	4.4 (0.4)	272 (10)
$\mu_0H=6$	5.6 (0.4)	165 (10)
(b) V_7Ni		
Field (T)	T_{peak} (K)	Height (emu S K $mol^{-1})^{-1}$
$\mu_0H=0.5$	3.1 (0.4)	725 (10)
$\mu_0H=1.5$	3.9 (0.4)	533 (10)
$\mu_0H=3.2$	–	–
$\mu_0H=6.18$	5.3 (0.4)	215 (10)

software or a home-made one. PHI is a computer program designed for the calculation of the magnetic properties of paramagnetic coordination complexes. It is based on the construction and diagonalization of the Hamiltonian matrix that describes the system under study, from which it is possible to obtain different variables of physical interest such as susceptibility, magnetization, heat capacity, and energy levels; see also Ref. [37]. (The preliminary results yielded $J=-4.64$ K for V_7Zn and $J=-4.12$ K for V_7Zn. See also Ref. [38].)

The behavior observed in vanadium rings is similar to the one observed in all semi-integer spin rings [13, 14]. As done for all magnetic molecules and rings, the NSLR data can be fitted by Eq. 5.

The solid lines in Fig. 7 are the best fit by using Eq. 5. For these fits, ω_c was assumed to be in the power law form ($\omega_c=CT^{\alpha}$) according to what was found in previous publications [13–19, 33]. The parameters used in the fit of Fig. 6 are: $A=1.9$ $(0.5)\times10^{11}$ rad^2mol/s^2 emu K, $C=3.1$ $(0.5)\times10^6$ rad/s, $\alpha=3$ (0.5) for V_7Zn, and $A=2$ $(0.5)\times10^{11}$ rad^2mol/s^2 emu K, $C=3.5$ $(0.3)\times10^6$ rad/s, $\alpha=3$ (0.5) for V_7Ni.

As seen in Fig. 7 the lowest field data are fitted well, while the higher fields data are not well reproduced as regards the amplitude of the peak value. To better compare the behavior of $1/T_1(T)$ experimental data at different applied magnetic fields with the BPP model of Eq. 5, we report in Fig. 8 for both V_7Ni and V_7Zn the height of the maximum of experimental $1/(T_1\chi T)$ vs. $1/\mu_0H$ (see data points in Table 3). These data are compared with the expected behavior from the exact fit of Eq. 5 using the parameters obtained on $\mu_0H=0.5$ T data for V_7Zn, represented by the solid line. As can be seen, the discrepancy is outside the experimental error. To make sure that the problem does not arise from the choice of the T dependence of the correlation frequency, we also tried to fit the data using an exponential dependence for ω_c i.e., $\omega_c = C\cdot\exp(\Delta/k_BT)$, where Δ is the energy gap between two electronic levels, but the quality of the fits did not improve. In addition, we also tried to fit our

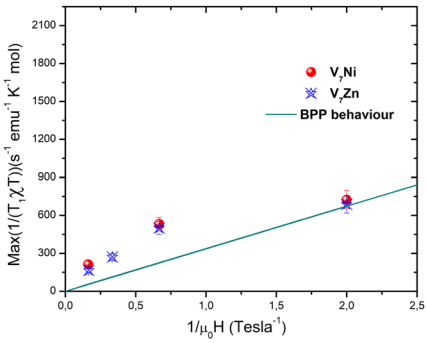

Fig. 8 Experimental height of the peaks of $1/(T_1\chi T)$ of V_7Zn and V_7Ni for the different values of the inverse magnetic field (scattered points), compared with the BPP behavior (solid line), calculated for V_7Zn by fitting the experimental data at $\mu_0 H = 0.5$ T

experimental data using a more refined model [16–19, 39, 40], where more than one correlation frequency determines the form of the spectral density of the electronic spin fluctuations, which thus results in a sum of Lorentzian functions pertaining to different correlation frequencies $\omega_c^{(i)}$. Even with a continuous distribution of correlation frequencies, it was not possible to fit the data (fitting curves not shown).

The observed discrepancy could signify that the spin–spin correlation function $G(t)$ is completely different from the simple exponential one assumed in Eq. 5 as a result of the difference between the electronic spins of V^{2+} ion ($s = 1$) with respect to the case of semi-integer spins. On the other hand, since the shape of the peak and the position of the maximum at different fields seem to be well reproduced by the usual model (Eq. 5), it is more likely that the height of the peak does not scale with $1/\mu_0 H$ as the consequence of the "wipe-out" effect. In fact, the NSLR data around the peak were collected in the temperature range in which there is a loss of ^{1}H NMR signal (see Fig. 6). It should be remarked that in this temperature range, we keep measuring the fast relaxing component and this fast component decreases in intensity with respect to the slow component (see Fig. 7), signaling that we are losing the fastest relaxing nuclei. Thus the value of the measured NSLR can be lower than what it would be if the fastest relaxing nuclei were detected, and this alters the height of the peak in the NSLR versus temperature in Fig. 7. As a matter of fact, an elaborate theoretical analysis on different rings has demonstrated that once the data are corrected for the "wipe-out" effect, they fit well Eq. 5 [22].

An important experimental result which is independent of the theoretical analysis is contained in the fact that, as shown in Fig. 7, the T and H dependence of NSLR in V_7Ni and V_7Zn are practically the same. Therefore, one could conclude that the spin dynamics in the intermediate temperature range ($T \sim J/k_B$) is not affected by the ground state spin value S_T and/or topological effects, since the V_7Zn and V_7Ni are "open, $S_T = 1$" and "closed, $S_T = 0$" spin-1 AFM ring, respectively.

5 Summary and Conclusion

The spin dynamics of two integer spin rings, V_7Zn and V_7Ni, were investigated through measurements of proton spin–lattice relaxation rate (NSLR) at room temperature as a function of the magnetic field, and as a function of temperature at

different applied magnetic fields. The purpose of the investigation is to compare the results in the present integer $s=1$ spin rings with the ones known in the literature for half integer spins, to find out if one can detect a different behavior between the quantum integer ($s=1$) and the ($s\geq 3/2$) semi-integer spin systems.

The experimental investigation was performed in two different temperature regions: (a) high temperature ($k_BT>>J$), where the magnetic moments in a spin system are weakly correlated and the system behaves like a paramagnet; (b) intermediate and low temperature ($k_BT\leq J$), where the evolution of the magnetic properties and the spin dynamics of the system reflects the progressive correlation among magnetic moments leading to a collective ground state at very low temperature.

At high temperature, the frequency (magnetic field) dependence of the proton NSLR indicates that the correlation function (CF) of the V^{+2} magnetic moments can be described by an initial fast decay due to the strong AFM interaction characterized by the exchange coupling constant J, followed by an intermediate time range with a slow decaying or constant CF and a final drop of the CF at a characteristic cutoff time. The intermediate time range is particularly interesting, since it is the consequence of the conservation of the total spin value for an isotropic Heisenberg finite size AFM ring, while the cutoff time (frequency) is due, e.g., to anisotropic terms in the spin Hamiltonian. In the two vanadium rings investigated, it was found that the behavior of the CF is very similar to the one observed in semi-integer spins [13, 14], but with a smaller cutoff frequency which allows to detect a narrow time range where the decay of the CF is described by a spin diffusion process.

At lower temperatures, the CF is ideally described by an exponential decay with a single dominating correlation time which describes the fluctuation of the collective modes of the magnetization. This CF generates a Lorentzian-type spectral density with a width which decreases on lowering the temperature, reflecting the slowing down of the collective fluctuations. The experimentally measured NSLR, renormalized by the effective magnetic moment χT, shows a characteristic magnetic field-dependent maximum as a function of temperature with a peak occurring at a temperature T_{max} of the order of the exchange constant ($kT_{max}\approx J$). The proton NSLR in the two vanadium rings have been fitted with the same formula used for semi-integer spins and the results are similar, although a very strong " wipe-out" effect present in the vanadium rings alters the intensity of the peaks revealed at all applied fields.

One can thus conclude that the present NMR study of the spin dynamics at high and intermediate temperature in $s=1$ vanadium rings does not show any detectable difference from the spin dynamics observed in semi-integer spin rings [13, 14]. The investigation regarding the detection of a difference in spin dynamical behavior between quantum integer spins and semi-integer spins in finite size rings, in view also of the Haldane gap effect, should be continued at much lower temperature and in vanadium rings with an increasing number of spins in the ring. Moreover, studies on homometallic closed or open V-based rings and with different parity (odd or even number of V ions) are envisioned, eventually making use of ^{51}V NMR to directly access spin dynamics from investigating the nuclei of the magnetic centers.

Acknowledgements Most work was developed under the FIRB Project No. RBFR12RPD1 of the Italian Ministry of Education and Research. Motorsport project by INSTM-Regione Lombardia, and EU-COST

projects EURELAX-15209 and MOLSPIN-15128 are also gratefully acknowledged. PA thanks the Department of Physics of the Università degli Studi di Milano for support. Two of us (A.L. and C.S.) take the occasion for a special thanks to Dante, who through his high level of human and professional support has strongly contributed to their career, and still represents a precious source of inspiration.

Funding Open access funding provided by Università degli Studi di Pavia within the CRUI-CARE Agreement.

References

1. D. Gatteschi, R. Sessoli, J. Villain, *Molecular Nanomagnets* (Oxford University Press, Oxford, 2011)
2. F. Haldane, Phys. Lett. A **93**, 464 (1983)
3. R. Sessoli et al., Nature **365**, 141 (1993)
4. B. Barbara et al., J. Magn. Magn. Mater. **140**, 1825 (1995)
5. L. Thomas et al., Nature **383**, 145 (1996)
6. J.R. Friedman et al., Phys. Rev. Lett. **76**, 3830 (1996)
7. A.A. Mukhin et al., Europhys. Lett. **44**, 778 (1998)
8. M.N. Leuenberger, D. Loss, Nature **410**, 789 (2001)
9. D. Stepanenko, M. Trif, D. Loss, Inorg. Chim. Acta **361**, 3740 (2008)
10. A. Conrad, P. Goodwin, F. Ortu, D. Reta, N.F. Chilton, D.P. Mills, Nature **548**, 439 (2017)
11. F.-S. Guo, B.M. Day, Y.C. Chen, M.L. Tong, A. Mansikkamäki, R. Layfield, Angew. Chem. Int. Ed. **56**, 11445 (2017)
12. R.H. Laye, F.K. Larsen, J. Overgaard, C.A. Muryn, E.J.L. McInnes, E. Rentschler, V. Sanchez, S.J. Teat, H.U. Güdel, O. Waldmann, G.A. Timco, R.E.P. Winpenny, Chem. Commun. **9**, 1125 (2005)
13. F. Borsa, A. Lascialfari, Y. Furukawa, in *Novel NMR and EPR Techniques*, ed. by J. Dolinsek, M. Vilfan, S. Zumer (Springer, New York, 2006) pp. 304–355
14. F. Adelnia, M. Mariani, L. Ammannato, A. Caneschi, D. Rovai, R. Winpenny, G. Timco, M. Corti, A. Lascialfari, F. Borsa, J. Appl. Phys. **117**, 17B308 (2015)
15. H. Amiri, A. Lascialfari, Y. Furukawa, F. Borsa, G.A. Timco, R.E.P. Winpenny, Phys. Rev. B **82**, 144421 (2010)
16. S.H. Baek, M. Luban, A. Lascialfari, E. Micotti, Y. Furukawa, F. Borsa, J. van Slageren, A. Cornia, Phys. Rev. B **70**, 134434 (2004)
17. P. Santini, S. Carretta, E. Liviotti, G. Amoretti, P. Carretta, M. Filibian, A. Lascialfari, E. Micotti, Phys. Rev. Lett. **94**, 077203 (2005)
18. I. Rousochatzakis, A. Lauchli, F. Borsa, M. Luban, Phys. Rev. B **79**, 064421 (2009)
19. A. Bianchi, S. Carretta, P. Santini, G. Amoretti, J. Lago, M. Corti, A. Lascialfari, P. Arosio, G. Timco, R.E.P. Winpenny, Phys. Rev. B **82**, 134403 (2010)
20. E. Garlatti, S. Carretta, P. Santini, G. Amoretti, M. Mariani, A. Lascialfari, S. Sanna, K. Mason, J. Chang, P. Tasker, E.K. Brechin, Phys. Rev. B **87**, 054409 (2013)
21. A. Abragam, *The Principles of Nuclear Magnetism* (Clarendon Press, Oxford, 1961)
22. C.P. Slichter, *Principles of Magnetic Resonance* (Springer-Verlag, New York, 1996), pp. 65–80
23. F. Carboni, M. Richards, Phys. Rev. **177**, 889 (1969)
24. D.G. McFadden, R.A. Tahir-Kheli, G. Bruce Taggart, Phys. Rev. **185**, 854 (1969)
25. F.B. McLean, M. Blume, Phys. Rev. B **7**, 1149 (1973)

26. G. Müller, Phys. Rev. Lett. **60**, 2785 (1988)
27. F. Borsa, M. Mali, Phys. Rev. B **9**, 2215 (1974)
28. J.P. Boucher, M. Ahmed Bakheit, M. Nechtschein, M. Villa, G. Bonera, F. Borsa, Phys. Rev. B **13**, 4098 (1976)
29. J. Tang, S.N. Dikshit, J.R. Norris, J. Chem. Phys. **103**, 2873 (1995)
30. J.H. Luscombe, M. Luban, F. Borsa, J. Chem. Phys. **108**, 7266 (1998)
31. F. Borsa, A. Rigamonti, in *Magnetic Resonance at Phase Transition*, ed. by Frank J. Owens, Charles P. Poole, Horacio A. Farach (Academic Press, New York, 1986) pp. 79–136
32. F. Adelnia, PhD dissertation, Università degli studi di Milano (Milano, Italy, 2016)
33. M. Belesi, A. Lascialfari, D. Procissi, Z.H. Jang, F. Borsa, Phys. Rev. B **72**, 014440 (2005)
34. T. Moriya, Prog. Theor. Phys. **16**, 23 (1956)
35. T. Moriya, Prog. Theor. Phys. **28**, 371 (1962)
36. N. Bloembergen, E.M. Purcell, R.V. Pound, Phys. Rev. **73**, 679 (1948)
37. N.F. Chilton, R.P. Anderson, L.D. Turner, A. Soncini, K.S. Murray, J. Comput. Chem. **34**, 1164 (2013)
38. A. Radaelli, MD thesis, Università degli studi di Milano (Milano, Italy, 2015)
39. D. Procissi, P. Arosio, F. Orsini, M. Marinone, A. Cornia, A. Lascialfari, Phys. Rev. B **80**, 094421 (2009)
40. T. Orlando, A. Capozzi, E. Umut, L. Bordonali, M. Mariani, P. Galinetto, F. Pineider, C. Innocenti, P. Masala, F. Tabak, M. Scavini, P. Santini, M. Corti, C. Sangregorio, P. Ghigna, A. Lascialfari, J. Phys. Chem. C **119**, 1224 (2015)

Affiliations

F. Adelnia[1] · P. Arosio[1] · M. Mariani[2] · F. Orsini[1] · A. Radaelli[3] · C. Sangregorio[4] · F. Borsa[2] · J. P. S. Walsh[5] · R. Winpenny[6] · G. Timco[4] · A. Lascialfari[1,2,7]

[1] Dipartimento di Fisica "A. Pontremoli" and INSTM RU, Università degli Studi di Milano, Milan, Italy

[2] Dipartimento di Fisica and INSTM RU, Università degli Studi di Pavia, Pavia, Italy

[3] Laboratory for Functional and Metabolic Imaging, EPFL, Lausanne, Switzerland

[4] Dipartimento di Chimica, ICCOM-CNR, Sesto Fiorentino, FI, Italy

[5] Department of Chemistry, University of Massachusetts Amherst, Amherst, MA, USA

[6] The Lewis Magnetism Laboratory, School of Chemistry, The University of Manchester, Manchester, UK

[7] Istituto di Nanoscienze, CNR-S3, Modena, Italy